

# Testing and Isolation Efficacy: Insights from a Simple Epidemic Model

May 12, 2021

## 1 Abstract

The effect of testing processes, including testing and test reporting, on an epidemic dynamics, involving infection and recovery, can be studied at the individual level or the community level (e.g., nursing homes, long-term-care facilities, etc.). Gaining insights to determine the sensitivity of the epidemic dynamics with respect to the testing processes will depend on underlying factors including the level of focus (individual or community), assumptions (model), and the interplay between these factors. In particular, the fast testing and test reporting may be beneficial at the community-level, supported by many studies, as it gives a rapid assessment of the situation, identifies hot spots, and may enable rapid contact-tracing. However, the potential advantage of a slow rate of test return on the dynamics of an epidemic is real, often neglected, and needs to be quantified. At the individual level, this advantage can manifest in the following sense: individuals awaiting their test results or who have tested positive may partially or fully self-isolate, thus reducing or eliminating their potential in the transmission process. In this paper, we investigated this individual-level effect of testing processes on the epidemic dynamics by developing a SIR-type model. Although the model development was motivated by the COVID-19 epidemic, the model has general epidemiological and testing structures. The realistic components of the model include *per capita* testing intensity, test sensitivity and specificity, rate of test return, and isolation efficacy in reduction of the probability of transmission. The novel component is the compartment-specific relative testing weights, which reflect the testing strategies—surveillance, diagnosis, or control. Here, we compare two testing strategies, random vs. targeted, and concluded that the targeted testing strategy is more effective in the sense that achieving reduction of  $\mathcal{R}_0$  can occur in a lower range of testing intensity and longer test return time relative to the random testing. Furthermore, we show that increasing *per capita* testing intensity and reducing the test return time would be beneficial on the dynamics of an epidemic in general but there are exception cases. In particular, it is possible for the basic reproduction number,  $\mathcal{R}_0$ , to be increasing with respect to the *per capita* testing intensity and the rate of test return.

## 2 Introduction

The observed dynamics of the COVID-19 epidemic are driven by both epidemiological processes (infection and recovery) and testing processes (testing and test reporting). In addition to shaping epidemic observations (via case reports), testing processes can also affect epidemiological dynamics. In particular, individuals with confirmed infections (positive tests) are likely to self-isolate, and individuals who are awaiting the results of a test may do so also (possibly to a lesser extent). We developed a mechanistic model that incorporates epidemic processes and testing in order to explore the effects of testing and isolation on epidemic dynamics.

If testing influences behavior, then epidemic dynamics will depend on patterns of who gets tested. The impacts of testing will depend on intensity (tests performed per day), and on how strongly testing is focused on people who are infectious. This level of focus depends in turn on the purpose and design of testing programs. When testing is done for the purposes of disease surveillance (Foddai et al., 2020) tests should be assigned randomly across the population, possibly with a stratified design for statistical efficiency (Graubard and Korn, 1996) [Ali: a better ref everyone?].

Over the course of the COVID-19 pandemic, however, the vast majority of testing has been done with other goals – primarily diagnosis (determining the infection status for clinical purposes), or control (determining the infection status in order to quickly isolate cases that have been found by contact tracing), which we characterize as *targeted* testing strategies. In these cases, testing probabilities vary widely across epidemiological compartments; in our dynamical model, we will characterize these probabilities by assigning a *per capita* testing weight to each compartment that determines the *relative* probability that an individual in that compartment will be selected for testing (see Methods).

When testing is used primarily for diagnosis it will focus on people with infection-like symptoms; thus the relative testing weights for infected people will depend on the relative probability of infected people having symptoms. For COVID-19 infection, the testing weights will depend on the relative asymptomatic infections, time spent pre-symptomatic vs. symptomatic infections – and also the incidence of COVID-19-like symptoms among people in the population *not* infected with COVID-19. Testing for epidemic control will focus on people who are known to have been in contact with known infected cases; in this case the testing weights for infected vs. uninfected people will depend on the probability of infection given contact, as well as the thoroughness and effectiveness of the system for identifying suspicious contacts.

The main interest from the epidemiological point of view is to know whether the number of infected individuals goes through an exponential growth phase, following the introduction of an infection in a totally susceptible population, before the disease becomes extinct. This is determined by studying the basic reproduction number  $\mathcal{R}_0$ . It is defined as the expected number of secondary infections arising from a typical infective individual in a completely susceptible population (Dietz, 1993). In the early stages of an epidemic the number of infected individuals is expected to grow exponentially over time when  $\mathcal{R}_0 > 1$ , and to decline over time when  $\mathcal{R}_0 < 1$ . Although the value of  $\mathcal{R}_0$  cannot completely characterize the dynamics of even the simplest epidemic model (Shaw and Kennedy, 2021), it does give a simple and widely accepted index for the difficulty of control, as well as some indication

of the likely final size of an epidemic (Ma and Earn, 2006).

In order to understand the effect of testing processes on an epidemic dynamics, we developed a mechanistic SIR-type model with epidemic and testing components. This model provides a sensible platform to link the modeling of epidemic and testing components and study their interaction. Here, we studied the the effect of testing intensity, rate of test return and the isolation efficacy in reduction of the probability of transmission on the epidemic dynamics when different levels of testing “focus” (from random to highly targeted) are in place. Our model provides insights to the sensitivity of the epidemic dynamics, through  $\mathcal{R}_0$ , with respect to the underlying testing and isolation parameters. [Ali: edited in response to David comments.]

### 3 Methods

We developed a deterministic model, Eqs. (A1), which groups individuals based on disease status and testing status. Disease states include Susceptible, Infectious and Recovered (thus this is an SIR-type model), and testing status categorizes people as *untested*, *waiting-for-positive*, *waiting-for-negative*, or *confirmed positive* (Fig. 1). Symbolically, the testing status of an individual in the disease compartment  $X$ , where  $X \in \{S, I, R\}$ , is reflected in the subscript, namely  $X_u$ ,  $X_p$ ,  $X_n$  and  $X_c$ , for *untested*, *waiting-for-positive*, *waiting-for-negative*, or *confirmed positive*, respectively. Note that the top-to-bottom order of the testing-based compartments of each disease-based compartment  $X$  in the flowchart (Fig. 1) and the model equations (A1) should match. However, we switched  $X_u$  and  $X_n$  in the flowchart (Fig. 1) for the sake of tidiness of the flowchart. Further, two ‘accumulator’ compartments,  $N$  and  $P$ , were also incorporated in the model in order to collect cumulative reported negative or positive tests. The model equations and details of calculation of the basic reproduction number  $\mathcal{R}_0$  are presented in the appendix (see Sec. 5.1).

Table 1 defines the model parameters, which are generally straightforward *per capita* flows between compartments, or modifiers to these flow rates. The novel component of the model comes in through the compartment-specific relative testing weights  $w_S$ ,  $w_I$  and  $w_R$ ; these give the relative rates at which people in the  $S$ ,  $I$ , and  $R$  compartments are tested, respectively. Thus, we can specify different levels of testing “focus” from random to highly targeted. For example,  $w_I/w_S = 3$  means that infected individuals are tested at three times the *per capita* rate of susceptible individuals.

In order to link to more applied models, we constructed this model so we could specify the total *per capita* testing rate. We do this by defining the weighted size of the testing pool  $W = w_S S_u + w_I I_u + w_R R_u$ , and calculating a scaling parameter for testing as:

$$\sigma = \frac{\rho N_0}{W}, \quad (1)$$

where  $\rho$  is the *per capita* testing intensity for population and defined as the number of daily tests taken in a population of size  $N_0$ . Thus, the *per capita* testing rate for compartment  $X$  is

$$F_X = \sigma w_X, \text{ where } X \in \{S, I, R\}. \quad (2)$$

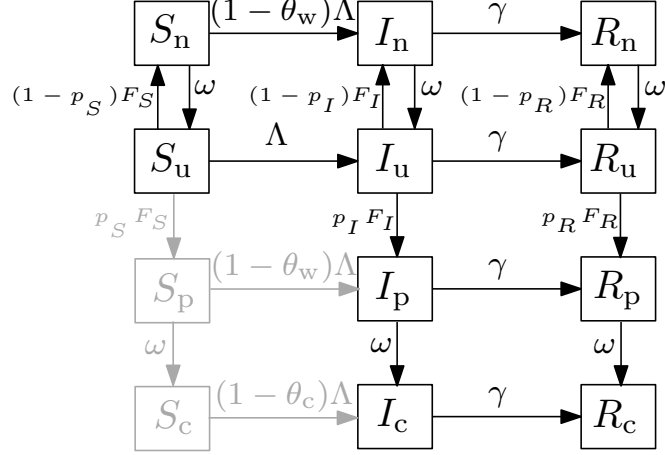


Figure 1: Flowchart of the SIR (Susceptible-Infectious-Recovered) model, A1. Here, the disease-based status of a compartment  $X$ , where  $X \in \{S, I, R\}$ , is combined with the testing-based status including  $X_u$ ,  $X_p$ ,  $X_n$  and  $X_c$ , for *untested*, *waiting-for-positive*, *waiting-for-negative*, or *confirmed positive*, respectively. Also,  $\Lambda$  is the force of infection with definition in Eq. (3),  $\gamma$  is the recovery rate,  $\omega$  is the rate of test return,  $F_X$  (defined in Eq. (2)) and  $p_X$  represent the *per capita* testing rate and the probability of positive tests, respectively, for compartment  $X$ . For further description of the parameters see Table 1.

For a high-sensitivity test, infected people typically flow through to the “confirmed positive” ( $I_c$ ,  $R_c$ ) compartments and are thus unavailable for further testing. Over the course of the epidemic, a fixed testing rate as specified in (1) can (if large enough) exhaust the pool of people available for testing, leading to a singularity when no one is left untested. Although this phenomenon does not affect our analysis of  $\mathcal{R}_0$ , it can affect the temporal dynamics (we discuss an adjustment to the model that solves this problem in the appendix).

The classical SIR model is based on the following implicit assumptions; well-mixed population, homogeneity of the population (i.e., all individuals are equally susceptible and equally infectious for the same length of time when infected), exponentially distributed duration of infection and large population size (see, e.g., Keeling and Rohani (2011)). In addition to these standard assumptions, our model assumes:

- (i) there is a single force of infection (new cases per unit time),  $\Lambda$ , defined as follows

$$\Lambda = \frac{\beta}{N_0} (I_u + (1 - \theta_w)(I_n + I_p) + (1 - \theta_c)I_c), \quad (3)$$

across all susceptible pools with transmission rate  $\beta$  and isolation efficacy in reduction of the probability of transmission for three testing-based compartments “waiting” and *confirmed positive* individuals,  $\theta_w$  and  $\theta_c$  respectively, (see Table 1 for further details),

- (ii) the efficacy of isolation is higher in confirmed individuals relative to the individuals awaiting test results. That is,

$$0 \leq \theta_w \leq \theta_c \leq 1.$$

Thus, for instance when the awaiting people follow the isolation perfectly,  $\theta_w$  is closer to 1, while when they less follow the isolation,  $\theta_w$  is closer to 0. For the simplicity of analysis, we also assume a perfectly specific test ( $p_S = 0$ ). This last assumption combined with the assumption that no susceptible individual is in waiting-for-*positive* or *confirmed positive* compartments, i.e.,  $S_p(0) = S_c(0) = 0$ , reduces the model to 10 equations where equations c and d in model (A1) are eliminated.

Symbol	Description	Unit	Value
$N_0$	Total population size	people	$10^6$
$\omega$	Rate of test return, i.e., rate of onward flow from “waiting” to “confirmed” or “untested” compartments	1/day	-
$\gamma$	Recovery rate	1/day	1/3
$\rho$	<i>per capita</i> testing intensity	1/day	-
$\theta_w$	Isolation efficacy in reduction of the probability of transmission for “waiting” individuals	-	-
$\theta_c$	Isolation efficacy in reduction of the probability of transmission for “confirmed positive” individuals	-	-
$\beta$	Transmission rate	1/day	0.339
$\Lambda$	Force of infection	1/day	-
$p_S$	Probability of positive tests for $S$ ( $= 1 - \text{specificity}$ )	-	0
$p_I$	Probability of positive tests for $I$ ( $= \text{sensitivity}$ )	-	1
$p_R$	Probability of positive tests for $R$ ( $= 1 - \text{specificity}$ )	-	0.5
$w_S, w_I, w_R$	Relative testing weights	-	Random: $\{1, 1, 1\}$ Targeted: $\{0.3, 1, 1\}$

Table 1: Parameters of the model (A1).

The Disease-Free Equilibrium (DFE) for the SIR model (Eqs. A1) is found by setting the infected compartments to 0 and solving for the unknowns. The DFE is

$$S_n^* = \frac{\rho}{\omega} N_0, \quad S_u^* = \frac{\omega - \rho}{\omega} N_0, \quad \text{and} \quad I_j = R_j = 0 \quad \text{for all } j. \quad (4)$$

The corresponding *per capita* testing rate (Eq. 2) for the infected compartment  $I$  at DFE is one of the key analysis parameters and can be simplified as

$$\hat{F}_I = (\omega\rho/(\omega - \rho))w_I/w_S. \quad (5)$$

The basic reproduction number,  $\mathcal{R}_0$ , was calculated by using the next-generation matrix method developed by van den Driessche and Watmough (2002). We present  $\mathcal{R}_0$  in the following form.

$$\mathcal{R}_0 = \frac{\beta}{\gamma}(1 - \Delta), \quad (6)$$

where the term  $\frac{\beta}{\gamma}$  is the classical basic reproduction number for a SIR model without testing and isolation (see, e.g., Keeling and Rohani (2011)), and the positive quantity  $\Delta$  is the “effectiveness of control” effectiveness of control due to testing and isolation processes defined as follows.

$$\Delta = \frac{1}{C N_0} (C_1 S_u^* + (C_2(1 - \theta_w) + C \theta_w) S_n^*), \quad (7)$$

where

$$C = (\omega + \gamma) (\gamma(\omega + \gamma) + (\gamma + \omega p_I) \hat{F}_I), \quad (8)$$

$$C_1 = (\omega + \gamma) (\theta_w \gamma + \theta_c \omega p_I) \hat{F}_I, \quad (9)$$

$$C_2 = (\omega \gamma (1 + p_I) \hat{F}_I + \gamma^2 (\omega + \gamma + \hat{F}_I)) \theta_w + \omega^2 p_I \hat{F}_I \theta_c. \quad (10)$$

Further details of derivation of  $\mathcal{R}_0$  are provided in appendix, Sec. 5.1. The explicit formula of  $\mathcal{R}_0$ , enables us to study the effect of parameters of interest, on  $\mathcal{R}_0$  mathematically and through numerical simulation. These parameters, i.e., parameters that could be manipulated by public-health policy include the isolation efficacy,  $\theta_c$  and  $\theta_w$ , *per capita* testing intensity,  $\rho$ , and the rate of test return,  $\omega$ . In particular, we look at the partial derivative of  $\Delta$  with respect to these parameters (see details in appendix, Sec. 5.2). It is notable that the derivative of  $\Delta$  with respect to  $\theta_w$ ,  $\theta_c$  and  $\rho$  was derived explicitly and for the whole domain of the parameter space. However, we analyzed the effect of  $\omega$  on  $\mathcal{R}_0$  for the case when testing intensity is very small relative to the population size,  $N_0$ . Specifically, we used the Taylor approximation of  $\Delta$  at  $\rho = 0$  to illustrate the unexpected nonmonotonic relationship between  $\mathcal{R}_0$  and  $\omega$ , and also to avoid unnecessary complicated computations for making this point.

The analytical calculation of the next-generation matrix and simplifying the expression of  $\mathcal{R}_0$  was carried out in Maple (Maplesoft, 2010). We used R (R Core Team, 2020) for simulations, in particular, for plotting the contours of  $\Delta$  (7) over a range of selected set of parameters of interest. The rest of model parameters kept fixed at sensible values (see Table 1 for the parameter values). Note that all plots are illustrated in the scale of the mean test return time  $1/\omega$  (day) and testing intensity  $\rho$  (1/day per 1000). Results are shown in Fig. 2 and Fig. 3 with two sets of panels; panel set (a) represents the random testing, identified by  $w_S = w_I = w_R = 1$ , and panel set (b) represents targeted testing, identified by  $w_S = 0.3$  and  $w_I = w_R = 1$ . Each panel set partitions a plot into a matrix of panels, namely facets, in which rows are specified by a value of  $\theta_w$  and columns are specified by a value of  $\theta_c$ . In our simulation,  $\theta_w$  and  $\theta_c$  vary in a discrete scale from 0 to 1 with 0.25 increment. Note that we are only plotting facets with  $\theta_w \leq \theta_c$  which is an assumption of our model.

To illustrate the changes in  $\mathcal{R}_0$  with respect to *per capita* testing intensity  $\rho$ , two sets of plots are presented. Fig. 2 reflects the changes in  $\mathcal{R}_0$  when  $\rho$  is small relative to the population size. Specifically,  $\rho \in [0, 0.013]$ , and the test return rate  $\omega \in [1/12, 2]$ . This is a more realistic scenario of testing as we have observed in COVID-19 pandemic. That

is, 1% of a population are tested per day at maximum capacity, so in a population of size  $N_0 = 10^6$ , 10000 individuals will be tested per day at maximum. In order to illustrate the non-monotonic changes in  $\mathcal{R}_0$  with respect to  $\rho$ , Fig. 3 with maximum capacity of  $\rho$  is larger relative to the population size,  $\rho \in [0, 1/5)$ , and the test return rate  $\omega \in [1/5, 2]$ . Note that the critical contour of  $\Delta = 1 - \frac{\gamma}{\beta}$ , corresponding to the threshold  $\mathcal{R}_0 = 1$ , is plotted in dotted line in the panels. Thus, a combination of  $\rho$  and  $\omega$  above this critical contour results in reducing  $\mathcal{R}_0$ . Also realize that  $\mathcal{R}_0 = \frac{\beta}{\gamma}$ , about 1.017 here, for the classical SIR model which can be achieved in the context of our model when no testing and no isolation are implied, that is  $\rho = 0$  or  $\theta_w = \theta_w = 0$ .

## 4 Results

Examining our formula for  $\mathcal{R}_0$  (6) gives the following results. See the appendix, Sec. 5.2, Sec. 5.3 and Sec. 5.6 for details.

1. Increasing the isolation efficacy parameters for tested and confirmed individuals decreases  $\mathcal{R}_0$ ;
2. Higher testing intensity  $\rho$  always decreases  $\mathcal{R}_0$  **if**: testing is random; **or**  $\rho$  is small.
3. A higher rate of test return always decreases  $\mathcal{R}_0$ , **if**  $\theta_w = 0$ .
4. Increasing testing “focus”  $\frac{w_I}{w_S}$  from random  $w_S = w_I$  to targeted  $w_S < w_I$  always decreases  $\mathcal{R}_0$ .

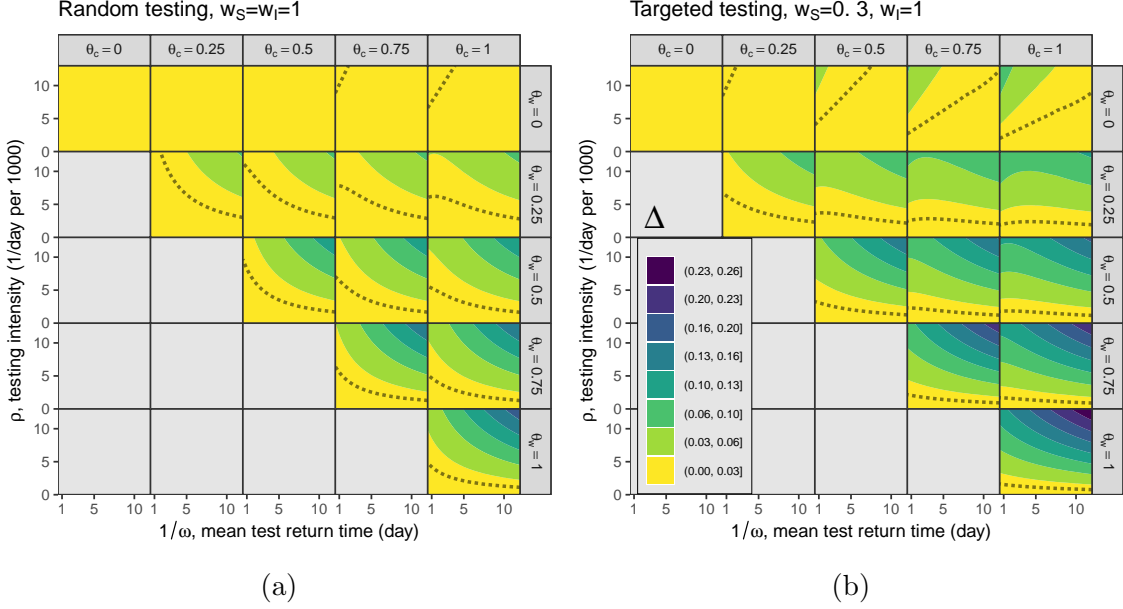


Figure 2: **A comparison of effectiveness control on  $\mathcal{R}_0$  at low level of *per capita* testing intensity  $\rho$ .** We numerically evaluate the effectiveness control parameter,  $\Delta$  (Eq. 7), with respect to testing and isolation. We use the following parameters (see Table 1 for a brief description):  $N_0 = 1 \times 10^6$ ,  $\omega \in [1/12, 2]$  1/day,  $1/\gamma = 3$  days,  $\rho \in [0, 0.013]$  1/day,  $\theta_w$  and  $\theta_c$  vary between 0 and 1 with 0 for no effect and 1 for the full effect of isolation on the transmission probability,  $\beta = 0.339$  1/day,  $p_S = 0$ ,  $p_I = 1$  and  $p_R = 0.5$ . Contours of  $\Delta$  are plotted for two testing strategies identified by a set of relative testing weights; (a) random testing where  $w_S = w_I = w_R = 1$  and (b) targeted testing where  $w_S = 0.3$  and  $w_I = w_R = 1$ . The black dotted line in each panel represents the critical contour of  $\Delta = 1 - \frac{\gamma}{\beta}$ , i.e., the  $\Delta$  corresponding to the threshold of  $\mathcal{R}_0 = 1$ .

Numerical results are shown in Figs. 2 and 3. When  $\theta_w = 0$  (top row of each panel), we see that shorter test-waiting times reduce  $\mathcal{R}_0$  ( $\Delta$  increases as we move to the left in each plot in this row). For non-zero  $\Delta$ , however, we mostly see the opposite effect: less waiting leads to more transmission. This is because returning negative tests leads people to stop distancing; this applies both to susceptibles, and to infectious people who receive negative test results because they were sampled when susceptible (or because of imperfect test sensitivity, which is not modeled in this figure).

We also see that greater test intensity  $\rho$  increases the effectiveness of control  $\Delta$  ( $\Delta$  increases as we move up in each plot in this Figure). Mathematically speaking, we did find a counter-vailing effect, but this can only be seen when we allow  $\rho$  to take unrealistically large values, and only for weighted/targeted testing (see Fig. 3). The explanation here is that more rapid testing leaves more susceptibles in the “waiting-for-no” category at the DFE; these people must then wait for their tests to be returned before they can be tested again, receive a positive test, and become cautious. This effect is usually weak compared to the helpful effects of testing, but if testing is weighted,  $\theta_w$  is low, and test returns are slow, it is possible for increasing  $\rho$  to reduce  $\Delta$  (see upper-right part of upper-right plot of Fig. 3(b)).



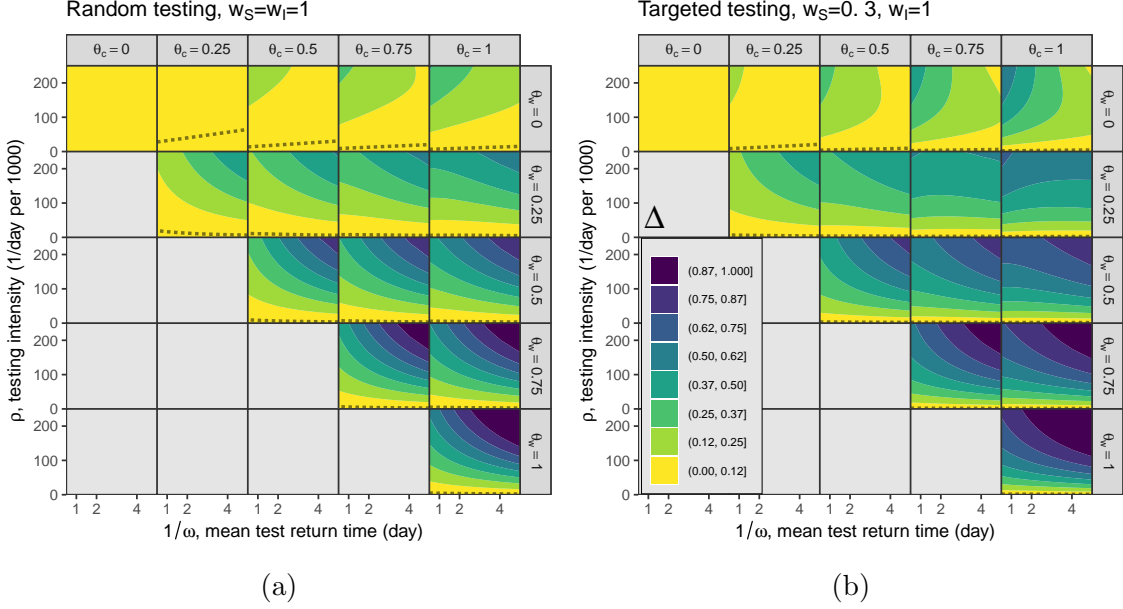


Figure 3: **A comparison of effectiveness control on  $\mathcal{R}_0$  at high level of *per capita* testing intensity  $\rho$ .** We numerically evaluate the effectiveness control parameter,  $\Delta$  (Eq. 7), with respect to testing and isolation. We use the following parameters (see Table 1 for a brief description):  $N_0 = 1 \times 10^6$ ,  $\omega \in [1/5, 2]$  1/day,  $1/\gamma = 3$  days,  $\rho \in [0, 1/5)$  1/day,  $\theta_w$  and  $\theta_c$  vary between 0 and 1 with 0 for no effect and 1 for full effect of isolation on the transmission probability,  $\beta = 0.339$  1/day,  $p_S = 0$ ,  $p_I = 1$  and  $p_R = 0.5$ . Contours of  $\Delta$  are plotted for two testing strategies identified by a set of relative testing weights; (a) random testing where  $w_S = w_I = w_R = 1$  and (b) targeted testing where  $w_S = 0.3$  and  $w_I = w_R = 1$ . The black dotted line in each panel represents the critical contour of  $\Delta = 1 - \frac{\gamma}{\beta}$ , i.e., the  $\Delta$  corresponding to the threshold of  $\mathcal{R}_0 = 1$ .

## 5 Discussion

### 1. A potential advantage of slow test reporting $\omega$ , result 3;

- Whether increasing  $\omega$  lowers  $\mathcal{R}_0$  depends on the precise combination of model parameters including  $\rho$ , testing strategies represented by compartment-specific testing weights, test sensitivity and specificity, and the level of isolation efficacy. - The potential advantage of slow test reporting is in the individual level as opposed to the community level, but seems unapplicable as a strategy. - May be this mechanism combined with increasing testing intensity  $\rho$  can be considered alongside other prevention methods, eg., social distancing etc, when the transmission is in the exponential-growth phase (in order to increase the generation interval). - One reason in favor of prolonging  $1/\omega$  is that it is easy to manipulate while increasing  $\rho$  can be limited to the resources.

### 2. The counter-vailing effect of *per capita* testing intensity, $\rho$ , on $\mathcal{R}_0$ ; - The explanation here is that more rapid testing leaves more susceptibles in the “waiting-for-no” $S_n$ category at the DFE and delay them to get to $I_c$ where they are subject to a full isolation, thus no transmission. - We are missing out on community-level

advantages of fast testing. - What is the explanation for having this counter-vailing effect of  $\rho$  in targeted testing and not in the random one? - May because in the targeted testing more  $I_u$ s are tested compared to  $S_u$ s, given that higher  $\omega$  leaves more people in  $S_n$  and  $I_n$  which results in more transission. - While targeted testing strategies, including targeting people with infection-like symptoms or the contacts of confirmed cases, are always more effective than random testing, as expected, we find that in some cases the direct effect of testing is that viral spread is greater for a slow test than for a fast test. This counter-intuitive effect can occur when people are cautious when awaiting a test result, and may not be robust to second-order effects of fast testing (such as better contact tracing).

### 3. Specifying the compartment-specific relative testing weights, Specifically $\frac{w_I}{w_S}$ ;

- More targeted testing is always good in viral control, - We incorporated the compartment-specific relative testing weights,  $w_S$ ,  $w_I$  and  $w_R$ , to model random testing and *targeted* testing strategies. Here, in the case of targeted testing and for the simplicity and illustration purposes, we assumed that infected and recovered individuals are tested at three times the *per capita* rate of susceptible individuals, thus  $w_I/w_S = 3$  and  $w_R = w_I$ . Note that we have not specified a methodology to assign particular relative testing weights corresponding to a particular targeted testing scenario. Modeling different targeted testing strategies, equivalently test-specific testing weights in our framework, requires prior information of the conditional probabilities of getting tested for people in a given compartment. This can be implied when we would like to quantify and compare the effect of different levels of test focus for infectious people on the basic reproduction number  $\mathcal{R}_0$ , and conclude about the disease spread management. For example, when people are tested for "screening", the individuals with potential higher mobility, eg. people who are getting on flights, get more tested and thus the coresponding heavier testing weight is assigned than people awaiting for a surgery and are probably going to stay in a long-term-care facility and consequently less mobile and more isolated to begin with. With our model, we would be able to compare the sensitivity of the disease dynamics, through  $\mathcal{R}_0$ , with respect to testing different high-risk groups in the population. This part needs to be developed further in future work.

### 4. What can we say in the context of strength and speed paradigm?

## References

- Dietz, K. (1993). The estimation of the basic reproduction number for infectious diseases. *Statistical methods in medical research*, 2(1):23–41.
- Foddai, A., Lubroth, J., and Ellis-Iversen, J. (2020). Base protocol for real time active random surveillance of coronavirus disease (COVID-19)–adapting veterinary methodology to public health. *One Health*, page 100129.
- Graubard, B. I. and Korn, E. L. (1996). Modelling the sampling design in the analysis of health surveys. *Statistical methods in medical research*, 5(3):263–281.

- 258 Keeling, M. J. and Rohani, P. (2011). *Modeling infectious diseases in humans and animals*.  
259 Princeton University Press.
- 260 Ma, J. and Earn, D. J. D. (2006). Generality of the final size formula for an epidemic of a  
261 newly invading infectious disease. *Bulletin of Mathematical Biology*, 68(3):679–702.
- 262 Maplesoft (2010). *Maple (14)*. a division of Waterloo Maple Inc., Waterloo, Ontario.
- 263 R Core Team (2020). *R: A Language and Environment for Statistical Computing*. R Foun-  
264 dation for Statistical Computing, Vienna, Austria.
- 265 Shaw, C. L. and Kennedy, D. A. (2021). What the reproductive number  $R_0$  can and cannot  
266 tell us about COVID-19 dynamics. *Theoretical Population Biology*.
- 267 van den Driessche, P. and Watmough, J. (2002). Reproduction numbers and sub-threshold  
268 endemic equilibria for compartmental models of disease transmission. *Mathematical bio-*  
269 *sciences*, 180(1-2):29–48.

## Appendix

### 271 5.1 Model and calculation of $\mathcal{R}_0$

The model in the form of a system of ordinary differential equations is

$$dS_u/dt = -\Lambda S_u - F_S S_u + \omega S_n, \quad (\text{A1a})$$

$$dS_n/dt = -(1 - \theta_w)\Lambda S_n + (1 - p_S)F_S S_u - \omega S_n, \quad (\text{A1b})$$

$$dS_p/dt = -(1 - \theta_w)\Lambda S_p + p_S F_S S_u - \omega S_p, \quad (\text{A1c})$$

$$dS_c/dt = -(1 - \theta_c)\Lambda S_c + \omega S_p, \quad (\text{A1d})$$

$$dI_u/dt = \Lambda S_u - F_I I_u + \omega I_n - \gamma I_u, \quad (\text{A1e})$$

$$dI_n/dt = (1 - \theta_w)\Lambda S_n + (1 - p_I)F_I I_u - \omega I_n - \gamma I_n, \quad (\text{A1f})$$

$$dI_p/dt = (1 - \theta_w)\Lambda S_p + p_I F_I I_u - \omega I_p - \gamma I_p, \quad (\text{A1g})$$

$$dI_c/dt = (1 - \theta_c)\Lambda S_c + \omega I_p - \gamma I_c, \quad (\text{A1h})$$

$$dR_u/dt = \gamma I_u - F_R R_u + \omega R_n, \quad (\text{A1i})$$

$$dR_n/dt = \gamma I_n + (1 - p_R)F_R R_u - \omega R_n, \quad (\text{A1j})$$

$$dR_p/dt = \gamma I_p + p_R F_R R_u - \omega R_p, \quad (\text{A1k})$$

$$dR_c/dt = \gamma I_c + \omega R_p, \quad (\text{A1l})$$

$$dN/dt = \omega(S_n + I_n + R_n), \quad (\text{A1m})$$

$$dP/dt = \omega(I_p + R_p), \quad (\text{A1n})$$

where parameters are specified in Table 1. The next generation matrix for this model is  $G = FV^{-1}$ , where matrix  $F$  represents the inflow of new infection to the infected compartments and matrix  $V$  represents the flow in the infected compartments when the population is totally susceptible. Matrices  $F$  and  $V$  are

$$F = \beta/N_0 \begin{bmatrix} S_u^* & (1 - \theta_w) S_u^* & (1 - \theta_w) S_u^* & (1 - \theta_c) S_u^* \\ (1 - \theta_w) S_n^* & (1 - \theta_w)^2 S_n^* & (1 - \theta_w)^2 S_n^* & (1 - \theta_w)(1 - \theta_c) S_n^* \\ 0 & 0 & 0 & 0 \\ 0 & 0 & 0 & 0 \end{bmatrix} \quad (\text{A2})$$

$$= \beta/N_0 \begin{bmatrix} S_u^* \\ (1 - \theta_w) S_n^* \\ 0 \\ 0 \end{bmatrix} [1, 1 - \theta_w, 1 - \theta_w, 1 - \theta_c], \text{ and} \quad (\text{A3})$$

$$V = \begin{bmatrix} \hat{F}_I + \gamma & -\omega & 0 & 0 \\ -(1 - p_I)\hat{F}_I & \omega + \gamma & 0 & 0 \\ -p_I\hat{F}_I & 0 & \omega + \gamma & 0 \\ 0 & 0 & -\omega & \gamma \end{bmatrix}. \quad (\text{A4})$$

The matrix inverse of  $V$  is

$$V^{-1} = \frac{1}{\gamma C} \begin{bmatrix} \gamma(\omega + \gamma)^2 & \gamma\omega(\omega + \gamma) & 0 & 0 \\ \gamma(\omega + \gamma)(1 - p_I)\hat{F}_I & \gamma(\omega + \gamma)(\hat{F}_I + \gamma) & 0 & 0 \\ \gamma(\omega + \gamma)p_I\hat{F}_I & \gamma\omega p_I\hat{F}_I & C\gamma/(\omega + \gamma) & 0 \\ \omega(\omega + \gamma)p_I\hat{F}_I & \omega^2 p_I\hat{F}_I & C\omega/(\omega + \gamma) & C \end{bmatrix}, \quad (\text{A5})$$

where  $C = (\gamma(\omega + \gamma) + (\gamma + \omega p_I)\hat{F}_I)(\omega + \gamma)$  and  $\hat{F}_I$  is the *per capita* testing rate for the infected people and represented in Eq. (5). Note that all the columns of matrix  $V^{-1}$  sum up to  $1/\gamma$ .

The particular form of  $F$  with two rows of zeros at the bottom results in the following blocked form of matrix  $G$ .

$$G = \begin{bmatrix} G_{11} & G_{12} \\ 0 & 0 \end{bmatrix}, \quad (\text{A6})$$

where both blocked matrices  $G_{11}$  and  $G_{12}$  are 2 by 2. Given the upper triangular form of matrix  $G$ , the basic reproduction number  $\mathcal{R}_0$  (defined as the spectral radius of matrix  $G$ ) is only determined by the blocked matrix  $G_{11}$ ,

$$G_{11} = \frac{\beta}{\gamma C} \begin{bmatrix} (\omega - \rho)/\omega \\ (1 - \theta_w)\rho/\omega \end{bmatrix} \begin{bmatrix} 1, 1 - \theta_w, 1 - \theta_w, 1 - \theta_c \end{bmatrix} \begin{bmatrix} \gamma(\omega + \gamma)^2 & \gamma\omega(\omega + \gamma) \\ \gamma(\omega + \gamma)(1 - p_I)\hat{F}_I & \gamma(\omega + \gamma)(\hat{F}_I + \gamma) \\ \gamma(\omega + \gamma)p_I\hat{F}_I & \gamma\omega p_I\hat{F}_I \\ \omega(\omega + \gamma)p_I\hat{F}_I & \omega^2 p_I\hat{F}_I \end{bmatrix}. \quad (\text{A7})$$

It is notable that matrix  $F$  (A2) has rank one and consequently  $G_{11}$  does so. That is  $G_{11}$  has only one non-zero eigenvalue which is  $\mathcal{R}_0$ .

The expression of  $\mathcal{R}_0$  has a complicated form with all of the model parameters involved. This expression can be simplified and represented given the specific form of matrix  $G_{11}$  (A7). For the purpose of simplicity we present  $\mathcal{R}_0$  in the manuscript in terms of expressions  $C$ ,  $C1$  and  $C2$ , specified in (8).

It remains hard to show that the reproduction number  $\mathcal{R}_0$  is decreasing with respect to *per capita* testing intensity,  $\rho$ , and the speed of the test return,  $\omega$ , for the feasible ranges of the parameters, that is

$$\omega > 0, \quad (\text{A8})$$

$$0 \leq \rho < \omega, \quad (\text{A9})$$

$$0 \leq \theta_w \leq \theta_c \leq 1, \quad (\text{A10})$$

$$\frac{w_I}{w_S} \geq 1. \quad (\text{A11})$$

One way to do such an analysis is based on the fact that  $\rho$  is *per capita* rate so for a large population size,  $N_0 \gg 1$ ,  $\rho$  is very small or close to 0, comparing to  $N_0$ . This provides a base to linearly approximate  $\mathcal{R}_0$  when  $\rho$  is close to 0, and use this approximation to analyze the behaviour of  $\mathcal{R}_0$  with respect to  $\omega$  (see section 5.3). In the next section we provide an equivalent representation of  $\mathcal{R}_0$  to provide a ground to prove that more testing intensity decreases  $\mathcal{R}_0$  for a general range of parameters.

## 5.2 More testing intensity may decreases $\mathcal{R}_0$

This is to provide a mathematical materials to prove that  $\frac{\partial}{\partial \rho} \Delta$  can be positive or negative, with  $\Delta$  defined in Eq. (8), and thus  $\frac{\partial}{\partial \rho} \mathcal{R}_0 < 0$ , where  $\mathcal{R}_0$  is the basic reproduction number, given in Eq. (6). We can rewrite matrix  $G_{11}$  in (A7) in the following form to simplify the calculations.

$$G_{11} = \frac{\beta}{\gamma C} \begin{bmatrix} S_u^*/N_0 \\ (1 - \theta_w) S_n^*/N_0 \end{bmatrix} [C - C_1, C - C_2], \quad (\text{A12})$$

where  $C$  is the same as the one in Eq. (8), i.e.,

$$C = (\omega + \gamma)(\gamma(\omega + \gamma) + (\omega p_I + \gamma) \hat{F}_I),$$

and  $C_1$  and  $C_2$  are

$$\begin{aligned} C_1 &= (\omega + \gamma)(\theta_w \gamma + \theta_c \omega p_I) \hat{F}_I, \\ C_2 &= (\omega \gamma (1 + p_I) \hat{F}_I + \gamma^2 (\omega + \gamma + \hat{F}_I)) \theta_w + \omega^2 p_I \hat{F}_I \theta_c, \end{aligned}$$

where  $\hat{F}_I$  is given in Eq. (5). Note that for analysis brevity, we let  $N_0 = 1$ , thus  $S_u^*$  and  $S_n^*$  are in the scale of 0 to 1.  $\mathcal{R}_0$  is in the same form as in Eq. (6)

$$\mathcal{R}_0 = \frac{\beta}{\gamma} (1 - \Delta),$$

where

$$\Delta = \frac{1}{C} (C_1 S_u^* + (C_2 (1 - \theta_w) + C \theta_w) S_n^*).$$

**The first goal** is to explore how changes in isolation,  $\theta_w$  and  $\theta_c$ , affects  $\mathcal{R}_0$ . Mathematically we would like to verify the sign of  $\frac{\partial \mathcal{R}_0}{\partial \theta_w}$  and  $\frac{\partial \mathcal{R}_0}{\partial \theta_c}$ . We start with simplifying  $\Delta$  (7) by factoring  $\theta_w$  and  $\theta_c$  in Eq. (7). Thus,  $\Delta$  can be rewritten as

$$\Delta = \frac{1}{C} \left( -D_1 S_n^* \theta_w^2 + (-\omega^2 p_I \hat{F}_I S_n^* \theta_c + D_2 S_n^* + \gamma \hat{F}_I (\omega + \gamma)) \theta_w + (\omega + \gamma S_u^*) \omega p_I \hat{F}_I \theta_c \right), \quad (\text{A13})$$

where

$$D_1 = (\omega + \gamma) \gamma^2 + (\omega + \gamma + \omega p_I) \gamma \hat{F}_I, \quad (\text{A14})$$

$$D_2 = (3\omega + 2\gamma) \gamma^2 + (\omega + \gamma + 2\omega p_I) \gamma \hat{F}_I + (\gamma + p_I \hat{F}_I) \omega^2. \quad (\text{A15})$$

$\Delta$ , Eq. (A13), is linear in  $\theta_c$  with a positive coefficient given by

$$1/C (\gamma S_u^* + \omega (1 - \theta_w S_u^*)) \omega p_I \hat{F}_I.$$

This results in increasing  $\Delta$ , thus decreasing  $\mathcal{R}_0$  with respect to  $\theta_c$ , that is  $\frac{\partial \mathcal{R}_0}{\partial \theta_c} \leq 0$ . Note that  $C$  is independant of  $\theta_c$  and  $\theta_w$ .

With a similar logic,  $\Delta$  (A13) is a concave-down quadratic equation in  $\theta_w$ , given by

$$1/C \left( -D_1 S_n^* \theta_w^2 + (-\omega^2 p_I \hat{F}_I S_n^* \theta_c + D_2 S_n^* + \gamma \hat{F}_I (\omega + \gamma)) \theta_w \right). \quad (\text{A16})$$

We show that the feasible range of  $\theta_w$  lies between 0 and the vertex of this parabola where the parabola is increasing in  $\theta_w$ , and so does  $\Delta$  which results in inferring  $\frac{\partial \mathcal{R}_0}{\partial \theta_w} \leq 0$ . It is enough to show that partial derivative of the expression (A16) with respect to  $\theta_w$  at  $\theta_w = 1$  is non-negative. It follows that

$$\left. \frac{\partial \Delta}{\partial \theta_w} \right|_{\theta_w=1} = 1/C \left( (D_2 - 2D_1 - \omega^2 p_I \hat{F}_I \theta_c) S_n^* + \gamma \hat{F}_I (\omega + \gamma) \right) \quad (\text{A17})$$

$$= 1/C \left( (\gamma(\omega + \gamma) + \gamma\omega^2 + (1 - \theta_c)\omega^2 p_I \hat{F}_I) S_n^* + \gamma(\omega + \gamma) \hat{F}_I (1 - S_n^*) \right), \quad (\text{A18})$$

which is a positive quantity, given that  $\theta_c$  and  $S_n^*$  vary between 0 and 1.

**The second goal** is to explore how changes in *per capita* testing intensity  $\rho$  affects  $\mathcal{R}_0$ . Mathematically we would like to verify the sign of  $\frac{\partial \mathcal{R}_0}{\partial \rho}$ , which specifically depends on  $\frac{\partial \Delta}{\partial \rho}$ . We use the derived expressions for  $S_u^*$  and  $S_n^*$ , given by Eqs. (4), in  $\Delta$  (7). Also, we define  $\phi = \hat{F}_S = \frac{\rho\omega}{\omega - \rho}$ , to reparametrize  $\rho$ . This is mainly to avoid singularity in  $\hat{F}_I$  (5), when testing intensity  $\rho$  is very close to the rate of test return  $\omega$ . Thus,  $\rho$  is reparametrized as

$$\rho = \frac{\omega\phi}{\omega + \phi}. \quad (\text{A19})$$

This one-to-one monotonic reparametrization enables us to simplify the mathematical expressions and explore the simpler  $\frac{\partial \Delta}{\partial \phi}$  instead of the complicated  $\frac{\partial \Delta}{\partial \rho}$ . The derivative is

$$\partial \Delta / \partial \phi = \frac{1}{d_3} (a_3 \phi^2 + b_3 \phi + c_3), \quad (\text{A20})$$

where

$$\begin{aligned} a_3 = \frac{w_I}{w_S} & \left( \left( (\theta_w p_I^2 - \theta_c p_I^2 \theta_w) \omega^3 + (2 \theta_w p_I^2 - \theta_c p_I^2 - p_I \theta_w^2 - \theta_c p_I \theta_w - p_I^2 \theta_w^2 + 2 \theta_w p_I) \gamma \omega^2 \right. \right. \\ & + (-2 p_I \theta_w^2 - \theta_c p_I + 3 \theta_w p_I - \theta_w^2 + \theta_w) \gamma^2 \omega + (\theta_w - \theta_w^2) \gamma^3 \Big) \frac{w_I}{w_S} + (-\theta_c p_I \theta_w + \theta_c p_I) \gamma \omega^2 + \\ & \left. \left. (\theta_w + \theta_c p_I - \theta_w^2 - \theta_c p_I \theta_w) \gamma^2 \omega + (\theta_w - \theta_w^2) \gamma^3 \right), \quad (\text{A21}) \right. \end{aligned}$$

$$b_3 = 2 \frac{w_I}{w_S} (\omega + \gamma) \gamma \left( (\omega + \gamma + \omega p_I) (2 - \theta_w) \gamma \theta_w + (1 - \theta_w) \omega^2 p_I \theta_c + \omega^2 p_I \theta_w \right), \quad (\text{A22})$$

$$c_3 = (\omega + \gamma)^2 \gamma \left( (2 - \theta_w) \gamma^2 \theta_w + \left( 1 + \frac{w_I}{w_S} \right) \omega \gamma \theta_w + \frac{w_I}{w_S} \omega^2 p_I \theta_c \right), \quad (\text{A23})$$

$$d_3 = \frac{(\omega + \gamma)}{\omega} \left( (\omega p_I + \gamma) \frac{w_I}{w_S} \phi + (\omega + \gamma) \gamma \right)^2 (\omega + \phi)^2. \quad (\text{A24})$$

Note that  $\phi \geq 0$ , also  $b_3$ ,  $c_3$  and  $d_3$  are all positive. However  $a_3$  can be positive or negative. If  $a_3 \geq 0$ ,  $\partial \Delta / \partial \phi \geq 0$  for all feasible range of parameters, thus  $\frac{\partial}{\partial \rho} \mathcal{R}_0 \leq 0$ . It is straight forward to show that  $a_3 \geq 0$  in case of random testing strategy, i.e.,  $w_S = w_I = 1$ . If  $a_3 < 0$ ,

then the quadratic expression in the numerator of (A20) has a positive root,  $\phi^*$ , such that for  $\phi > \phi^*$ ,  $\partial\Delta/\partial\phi < 0$ .

An example of this counter-vailing effect of  $\phi$ , and consequently  $\rho$ , on  $\mathcal{R}_0$  occurs when  $\theta_w = 0$  and  $\theta_c = 1$ . This is illustrated in the top-right panel of the Fig. 3 panel (b), where the strength of isolation for awaiting people is the least, but the most for the confirmed cases. In this case

$$a_3 = \frac{w_I}{w_S} \omega \gamma p_I ((\omega + \gamma) - \frac{w_I}{w_S} (\omega p_I + \gamma)).$$

Specifically, in the case of targeted testing which is identified with  $\frac{w_I}{w_S} > 1$ , and using a perfect sensitive test, thus  $p_I = 1$ , there exists a range for  $\rho$  over which  $\frac{\partial\mathcal{R}_0}{\partial\rho} \leq 0$ . Note that  $\rho$  and  $\omega$  have a similar mechanism in delaying people to get into  $I_c$ , thus we would expect to see the non-trivial counter-vailing effect of these two parameters on  $\mathcal{R}_0$ .

### 5.3 rate of returning tests

**The third goal** is to explore how changes in the rate of test return  $\omega$  affects  $\mathcal{R}_0$ . Mathematically we would like to verify the sign of  $\frac{\partial\mathcal{R}_0}{\partial\omega}$ , which specifically depends on  $\frac{\partial\Delta}{\partial\omega}$ . We use the linearization of  $\mathcal{R}_0$  around  $\rho = 0$  to show that there a non-monotonic relationship between  $\mathcal{R}_0$  and  $\omega$ . The Taylor expansion of  $\Delta$  at  $\rho = 0$  is

$$\Delta = \frac{\rho}{\omega \gamma (\omega + \gamma)} \left( \frac{w_I}{w_S} \omega^2 p_I \theta_c + \left( \frac{w_I}{w_S} + 1 \right) \gamma \omega \theta_w + \gamma^2 \theta_w (2 - \theta_w) \right). \quad (\text{A25})$$

This results in

$$\frac{\partial\Delta}{\partial\omega} = \frac{\rho}{\omega^2 (\omega + \gamma)^2} \left( \left( p_I \frac{w_I}{w_S} \theta_c - \left( 1 + \frac{w_I}{w_S} \right) \theta_w \right) \omega^2 + 2 \theta_w \gamma (\theta_w - 2) \omega + \theta_w \gamma^2 (\theta_w - 2) \right), \quad (\text{A26})$$

around  $\rho = 0$ . **[Ali: I stoped here!]**

Perhaps counter-intuitively, the equation above does not predict that  $\mathcal{R}_0$  is monotone decreasing with respect to  $\omega$ . In other words; our model does not predict that returning test results more rapidly *always* lower  $\mathcal{R}_0$ . In order to gain insight into this intriguing behavior, we examine the zeroes of  $\frac{\partial\mathcal{R}_0}{\partial\omega}(\omega)$ . Defining the following quantity,  $Q$ , will help us write the roots of  $\partial\mathcal{R}_0/\partial\omega$  neatly as follows.

$$Q = \frac{w_I}{w_S} \left( 1 - \frac{n_t - 1}{n_w - 1} p_I \right). \quad (\text{A27})$$

With that in mind, we can write the roots of  $\partial\mathcal{R}_0/\partial\omega$  as

$$\omega_1 = \frac{\gamma}{-\sqrt{1-Q}-1} \quad (\text{A28})$$

$$\omega_2 = \frac{\gamma}{\sqrt{1-Q}-1}. \quad (\text{A29})$$

Note that the zeroes are real if and only if  $Q < 1$ . Note that have  $\theta_c > \theta_w$ , so if  $p_I \approx 1$ , we will have  $Q < 0 < 1$ . Thus, if we assume near-perfect test sensitivity,  $\omega_1$  and  $\omega_2$  will be real.



Assuming  $\omega_1, \omega_2$  are real, it is easy to confirm that  $\omega_1 < 0$  by looking at the denominator. To see that  $\omega_2 > 0$ , recall that  $Q < 0$ , so  $\sqrt{1-Q} > 1$  and so  $\sqrt{1-Q} - 1 > 0$ . Knowing that  $\omega_1 < 0$ , the only root of interest (i.e., biologically relevant quantity) is  $\omega_2$ .

We can prove that  $\partial\mathcal{R}_0/\partial\omega > 0$  when  $\omega \in (0, \omega_2)$  and  $\partial\mathcal{R}_0/\partial\omega < 0$  when  $\omega \in (\omega_2, \infty)$  by computing the limits of  $\partial\mathcal{R}_0/\partial\omega$  at 0 and  $\infty$  respectively. So it follows that  $\mathcal{R}_0$  has a global maximum with respect to  $\omega$  at  $\omega = \omega_2$ .

Now we want to characterize the parameter regions on which  $\partial\mathcal{R}_0/\partial\omega < 0$  (i.e., the conditions under which returning test results more rapidly is favorable). By the previous analysis, this is equivalent to solving for  $\omega > \omega_2$ . So

$$\begin{aligned}\omega &> \omega_2 \\ \omega &> \frac{\gamma}{\sqrt{1-Q}-1} \\ \sqrt{1-Q} &> \frac{\gamma}{\omega} + 1\end{aligned}\tag{A30}$$

$$1-Q > \left(\frac{\gamma}{\omega} + 1\right)^2.\tag{A31}$$

Substituting in  $Q$  from (A27) we have

$$1 - \frac{w_I}{w_S} \left(1 - \frac{n_t - 1}{n_\omega - 1} P_i\right) > \left(\frac{\gamma}{\omega} + 1\right)^2\tag{A32}$$

$$- \frac{w_I}{w_S} \left(1 - \frac{n_t - 1}{n_\omega - 1} P_i\right) > \left(\frac{\gamma}{\omega} + 1\right)^2 + 1\tag{A33}$$

$$\frac{w_I}{w_S} \left(\frac{1 - n_t}{1 - n_\omega} P_i - 1\right) > \left(\frac{\gamma}{\omega} + 1\right)^2 + 1.\tag{A34}$$

Since all steps in deriving (A34) are reversible, (A34) gives a necessary and sufficient condition for  $\omega > \omega_2$ , which characterizes when returning tests more rapidly would cause a decrease in  $\mathcal{R}_0$ .

## 5.4 On Testing Rate and Numerical Singularity

In this work, we didn't do any numerical solutions for the trajectories in our analysis. However, if one tries to do so there would be a singularity issue to deal with. Specifically, the numerical singularity issue with the chosen  $\sigma$  (1) is that the population in  $S$  compartments appeared to blow up when the DFE is achieved. This is once the only untested people are susceptibles, the FOI will become  $\Lambda = 0$ , testing rate  $F_s = \rho N_0/S_u$ . Thus, the first equation of the model (A1) will become  $dS_u/dt = -\rho N_0 + \omega S_u$ . Thus changes in  $S_u$  will be no longer dependent on  $S_u$  with a linear rate of leaving the  $S_u$  compartment. IN fact the testing rate,  $\sigma$ , should be formulated such that people from the untested compartments will not be tested if they are not there. One way to fix this issue, is to consider a maximum testing rate,  $\tau$  (1/day). In general, we want to test at a rate of  $\rho$  across the whole population. This won't always be possible, so we impose a maximum rate of  $\tau$  per testable person and redefine  $\sigma = \frac{\tau \rho N_0}{\tau W + \rho N_0}$ , with the assumption that  $\tau \gg \rho$ . This alteration in  $\sigma$ , does not change any results related to  $\mathcal{R}_0$ , thus we only impose it in the simulation of the epidemic dynamic.

## 5.5 Expensive vs. cheap tests

The use of tests cheaper than RT-PCR has been proposed as a potential strategy for containing the COVID-19 pandemic. While cheaper tests may be less sensitive and reliable than RT-PCR, they allow for broader and more intense testing. In the analysis below, we compare the  $\mathcal{R}_0$  predicted by our model depending on the testing strategy.

Consider a test that allows us to test at rate  $\rho_1$  and has sensitivity  $P_{i,1}$ , and another test that allows us to test at  $\rho_2$  and has sensitivity  $P_{i,2}$ . Suppose that  $\rho_1 > \rho_2$ . Recall that the linearization of  $\mathcal{R}_0$  around  $\rho \approx 0$  is given by

$$\mathcal{R}_0 \approx \beta/\gamma + \frac{\beta\rho}{\omega(\omega + \gamma)\gamma^2 w_S} \left( \gamma(-\theta_w)(\gamma w_S + \omega w_I) + (-\theta_c)p_I w_I \omega^2 \right).$$

Treating  $\mathcal{R}_0$  as a function of  $\rho$  and  $P_i$ , we can reduce the inequality

$$\mathcal{R}_0(\rho_2, p_{I,2}) < \mathcal{R}_0(\rho_1, p_{I,1})$$

into

$$\begin{aligned} & \rho_1 \left( \gamma(-\theta_w)(\gamma w_S + \omega w_I) + (-\theta_c)p_{I,1} w_I \omega^2 \right) - \rho_2 \left( \gamma(-\theta_w)(\gamma w_S + \omega w_I) + (-\theta_c)p_{I,2} w_I \omega^2 \right) > 0 \\ & \vdots \\ & \frac{\rho_2 P_{i,2} - \rho_1 P_{i,1}}{\rho_1 - \rho_2} > \frac{\theta_w}{\theta_c} \cdot \frac{\gamma(\gamma w_S + \omega w_I)}{\omega^2 w_I} \end{aligned} \quad (\text{A35})$$

Note that the RHS is positive, thus a necessary condition for the inequality above to hold is that  $\rho_2 P_{i,2} > \rho_1 P_{i,1}$ , equivalently

$$\frac{P_{i,2}}{P_{i,1}} > \frac{\rho_1}{\rho_2}. \quad (\text{A36})$$

To state an example of this, if test  $A$  is three times as expensive as test  $B$  (and hence one can test three times as many people with test  $B$ ), using test  $A$  rather than  $B$  will be favorable only if test  $A$  is at least 3 times more sensitive than test  $B$ . Note that this is a necessary but not sufficient condition, so even if test  $A$  is three times more sensitive, it is still possible for test  $B$  to be more effective.

Eq. (A35) tells us precisely when a test corresponding to  $\rho_2, P_{i,2}$  will yield a lower  $\mathcal{R}_0$  than a test corresponding to  $\rho_1, P_{i,1}$ , where  $\rho_1 > \rho_2$ . Some of the qualitative *trends* that favor test 2 (the higher-sensitivity test) include

- individuals who test positive self-isolate much more than individuals who are waiting for their test result.
- the time it takes to return tests is much shorter than the mean infectious period.
- the testing intensity is much greater for infected individuals than susceptible individuals.

## 372 5.6 The effect of testing focus parameter $\frac{w_I}{w_S}$ on $\mathcal{R}_0$

We define  $w_{IS} = \frac{w_I}{w_S}$ .

$$\frac{\partial \Delta}{\partial w_{IS}} = \frac{(\omega - \rho) (\omega(\omega - \rho\theta_w) + \gamma(\omega - \rho)) (\theta_w\gamma + \theta_c\omega p_I)}{(-\omega^2\gamma + \omega\gamma\rho - \gamma\rho\omega w_{IS} - \omega\gamma^2 + \gamma^2\rho - \omega^2 p_I\rho w_{IS})^2}, \quad (\text{A37})$$

373 which is a positive quantity. Thus,  $\frac{\partial \mathcal{R}_0}{\partial w_{IS}} \leq 0$ . Therefore, increasing the focus of testing on  
 374 the infectious people will result in less transmission.